From Modal Mixing to Tunable Functional Switches in Nonlinear Phononic Crystals

R. Ganesh* and S. Gonella†

Department of Civil, Environmental, and Geo- Engineering, University of Minnesota, Minneapolis, Minnesota 55455, USA

(Received 9 October 2014; published 3 February 2015)

We introduce a paradigm for spatial and modal wave manipulation based on nonlinear phononic crystals and explore its potential for engineering wave control systems with tunable, adaptive, and multifunctional characteristics. Our approach exploits nonlinear mechanisms to stretch the frequency signature of the wave response and distribute it over multiple modes, thereby activating a mixture of modal characteristics and enabling functionalities associated with high-frequency optical modes, even while operating in the low-frequency regime. To elucidate the versatility of this approach, we consider different granular crystal configurations that span the available landscape of crystal topologies and wave control functionalities. The ability to switch between complementary functionalities allows rethinking nonlinear phononic crystals as programmable acoustic ports that form the building blocks of a new structural logic framework enabled by nonlinearity.

DOI: 10.1103/PhysRevLett.114.054302 PACS numbers: 43.25.+y, 45.70.-n, 46.40.Cd

Phononic crystals (PCs) are synthetic structural materials made of periodic sequences of unit cells and capable of performing spectral and spatial manipulation of acoustic and elastic waves. The hallmark feature of PCs is the ability to develop phononic band gaps, which makes them excellent acoustoelastic filters [1,2]. The material and geometric properties of the unit cell control the band gap distribution, thereby providing multiple avenues to achieve the desired filtering properties [3–5]. PCs also display frequency-dependent directivity [6], a property that can be exploited for the design of directional actuators and sensors [7].

A major drawback of linear phononic crystals lies with their inherent passivity, whereby the band structure and directional behavior are typically fixed for a given design. A promising avenue to achieve tunability is through the activation of nonlinear mechanisms. Along these lines, PCs made of soft elastomeric material have been shown to undergo reversible changes in band structure and directionality as a result of pattern transformations triggered by the activation of instabilities through the application of static compressive loads [8–10].

Another route to achieve tunability is via granular phononic crystals (GPCs) [11]. While the bulk of the work on granular crystals has been focused on one-dimensional chains, with special emphasis placed on localized wave modes such as solitons and breathers [12–14], recent efforts have investigated the behavior of 2D and 3D configurations [15–17]. The inherent tunability of granular systems has led to the proposition of a variety of metamaterial concepts such as tunable acoustic lenses and rectifiers [18–20]. The ability of GPCs to yield amplitude-dependent dispersion relations has also been explored for the design of tunable mechanical filters [21,22].

In contrast, the potentials of nonlinearity as a vehicle to activate tunable spatial directivity (the ability to tune the *spatial* characteristics of wave motion to specific operating conditions) have only been marginally explored. In this Letter, we demonstrate the potential of nonlinearity as a tool to achieve controllable spatial and modal wave manipulation, and we will introduce a strategy to engineer phononic crystals that can function as programmable acoustoelastic ports with tunable, adaptive, and multifunctional characteristics. We will first illustrate the idea using a simple abstract model and then extend the concept to GPC architectures with different topological complexity.

Consider the nonlinear spring-mass system shown in Fig. 1(a). The potential energy of the springs is assumed to have a nonlinear (cubic in this case) dependence upon the change in length. The displacements of the masses, which determine the change in length of the spring, are assumed to be small with respect to the initial unstretched length of the springs, thereby allowing a linearization of the geometric nonlinearity. Therefore, the equations of motion can be written as

$$\mathbf{M}\ddot{\mathbf{u}} + \mathbf{K}\mathbf{u} + \varepsilon \mathbf{f}_{\mathrm{NL}}(\mathbf{u}) = 0, \tag{1}$$

where $\mathbf{u}$ is a vector of displacements, $\mathbf{M}$ and $\mathbf{K}$ are the mass and linear stiffness matrices, respectively, and $\mathbf{f}_{\mathrm{NL}}$ is a force vector which has a nonlinear (quadratic in this case) dependence on the displacements. The weakness of the nonlinear term follows from the assumption of small displacements of the masses with respect to the length scale of the system [$u/L \approx \mathcal{O}(\varepsilon)$]. The angle of the cross-links is 45°, and, for simplicity, all the parameters of the system (masses, initial lengths of springs, and linear and nonlinear spring coefficients) are taken to be unity. The system is analyzed numerically and excited with a narrow-band seven-cycle Hann-modulated sine burst, which allows probing specific frequency ranges of the crystal [23,24].

If we assume very small displacements, the nonlinear term can be completely neglected, and oscillatory solutions of the form $Ae^{i(\xi n-\Omega t)}$ result in an eigenvalue problem which determines the dispersion relation between the frequency Ω and the wave number ξ [dashed curves in Figs. 1(b) and 1(c)]. Because of the dispersive nature of the system, propagating wave packets also feature an envelope modulation which occurs in a slower spatiotemporal scale than that of the carrier oscillation [25]. When the amplitude of the excitation is large enough that the effect of nonlinearity is no longer negligible, a more complex modulation of the packet envelope is observed. In the case of quadratic nonlinearity, the envelope modulation is modeled by the well-known nonlinear Schrödinger equation [26] and results in a long-wavelength component (referred to as an asymmetric envelope soliton), whose spectral content does not depend on the excitation frequency [23].

As we further increase the amplitude, the nonlinear term induces effects in the same spatiotemporal scale of the incident excitation which result in the generation of higher order harmonics [27]. For dispersive systems featuring multiple modes, the possibility to propagate higher harmonics is dictated by the availability of dispersion branches in the frequency range of the activated harmonics [28]. In this system, it is possible to choose frequencies belonging to the range of the acoustic branch such that the nonlinearity produces second harmonics that belong to the frequency range of the optical branch. As a result, the component of the response with frequency content corresponding to the second harmonic *hops* from the acoustic to the optical mode. This is illustrated in Figs. 1(b) and 1(c), in which the spectral content of the wave is shown for two different amplitudes and superimposed to the dispersion curves. For low amplitudes, the response only engages the acoustic mode, as shown in Fig. 1(b). As the amplitude of excitation is increased, we also observe the spectral signature of the second harmonic [Fig. 1(c)], which lies on the optical branch.

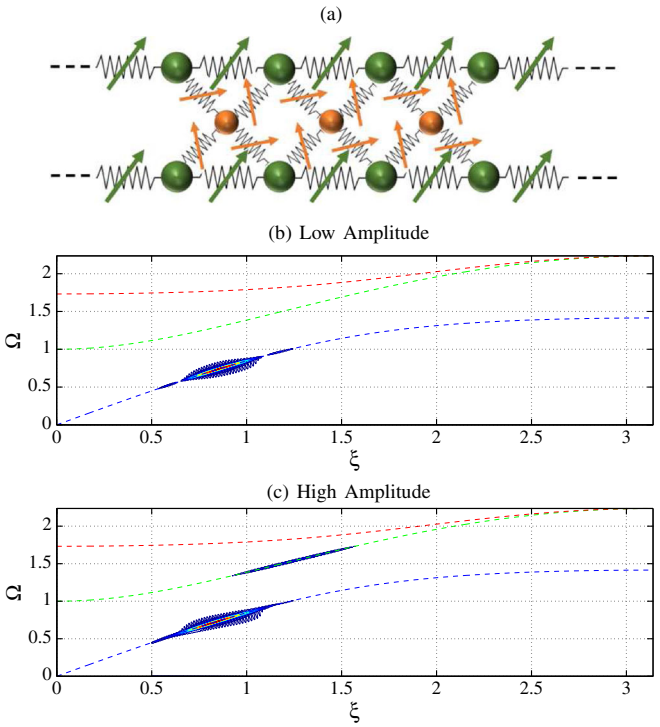

FIG. 1 (color online). Proof of mode hopping. (a) Schematic of 1D nonlinear crystal waveguide. (b),(c) Spectra of response for low and high amplitudes of excitation. The high-amplitude case displays the hopping mechanism resulting in the activation of the optical mode for an excitation applied in the acoustic range.

Since each branch of the dispersion relation is associated with a specific mode shape (which dictates the deformation of the unit cell and can be approximately determined from the eigenvectors of the linear model), the activation of the second harmonic by branch hopping yields an output signal with a broader frequency spectrum that stretches over multiple branches and blends the deformation characteristics of multiple modes (*modal mixing*). In this system, for example, the acoustic mode is characterized by in-phase dynamics between the top and bottom particle layers, which correspond to axial (longitudinal) deformation in the waveguide. In contrast, the optical mode activates out-of-phase dynamics between the layers, which result in the activation of shear horizontal deformation. These contrasting deformation patterns are indeed observed in Fig. 2, which shows a snapshot of the spatial profile of the wave packet. The packet features two distinct oscillatory components (both modulated by the asymmetric envelope): a faster, dominant feature and a slower, secondary contribution, whose difference in speed corresponds to the slight

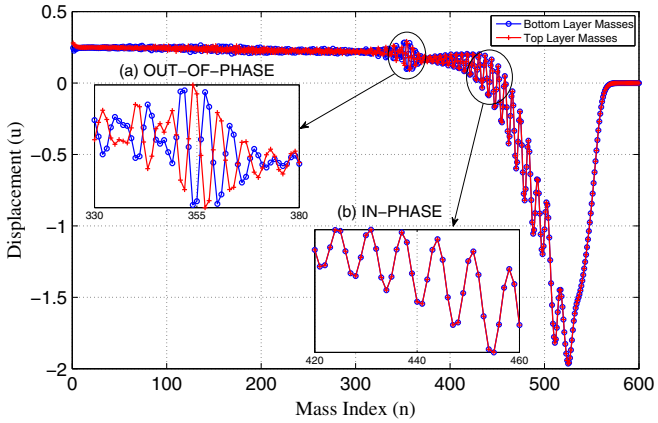

FIG. 2 (color online). Proof of concept of modal mixing. Snapshot of a wave packet revealing the coexistence of a faster acoustic mode (fundamental harmonic) and a slower optical mode (second harmonic). (a) The second harmonic response displays out-of-phase dynamics and shear deformation between top and bottom layers. (b) The fundamental harmonic response displays in-phase dynamics and axial (longitudinal) deformation. The displacement is normalized by the maximum excitation amplitude.

gap in group velocity between the two dispersion branches at the hopping point. We also observe that the layers indeed exhibit in-phase dynamics in the faster harmonic [Fig. 2(b)] and out-of-phase dynamics in the slower harmonic [Fig. 2(a)], in accordance with the mode shapes.

In summary, the waveguide behaves as an amplitude-controlled switch between two distinct operating modalities. For sufficiently weak excitations, the energy travels along the waveguide with high speed and primarily axial deformation, while larger amplitudes induce a partial energy migration to a slower mode that shears the structure horizontally. Therefore, by simply controlling the amplitude, we have access to deformation patterns and modal attributes that are typical of the optical mode, even while we excite the system in the low-frequency regime.

The availability of mode hopping and modal mixing mechanisms extends to any system that can be formally described by Eq. (1). The assumption of small displacements allows in fact a multiple-scale expansion of the equations of motion. As the amplitude of excitation is increased, the higher order terms in the solution become significant and give rise to higher harmonic contributions. Since the homogeneous part of the equations at every order of expansion have the same form [29], the solution at each order can be expressed as a linear combination of the eigenmodes of the corresponding linear system, thus establishing the mode shapes associated with the nonlinearly generated harmonics. In order to demonstrate the versatility of this general paradigm, we now revisit the concept using 1D and 2D granular phononic crystals with different topologies. It is worth recalling that, for sufficiently precompressed crystals, the nonlinearity due to the Hertzian contacts can be approximated by an equivalent quadratic nonlinearity [24], thus realizing a formal analogy with the spring-mass model discussed above.

Let us consider a granular waveguide consisting of two monoatomic chains cross-linked by an intermediate layer of stiffer spheres (e.g., aluminum and steel). An appropriate choice of the bead diameters [Fig. 3(a)] results in a configuration which can be viewed as a rectangular lattice with interstitial inclusions featuring only one tiling in the vertical direction. The system is precompressed in the horizontal and vertical directions to ensure that the beads remain in contact, and the excitation is applied at the first bead of the lower layer. We still constrain wave motion along the horizontal direction, but we allow each mass to have 2 degrees of freedom (horizontal and vertical displacement) to accommodate axial and flexural wave motion. The linearized dispersion relation features six branches, the lowest four of which are depicted in Fig. 3(b) [30]. Although, in general, the eigenmode shapes entail simultaneous activation of both horizontal and vertical degrees of freedom, certain modes predominantly excite one direction of motion.

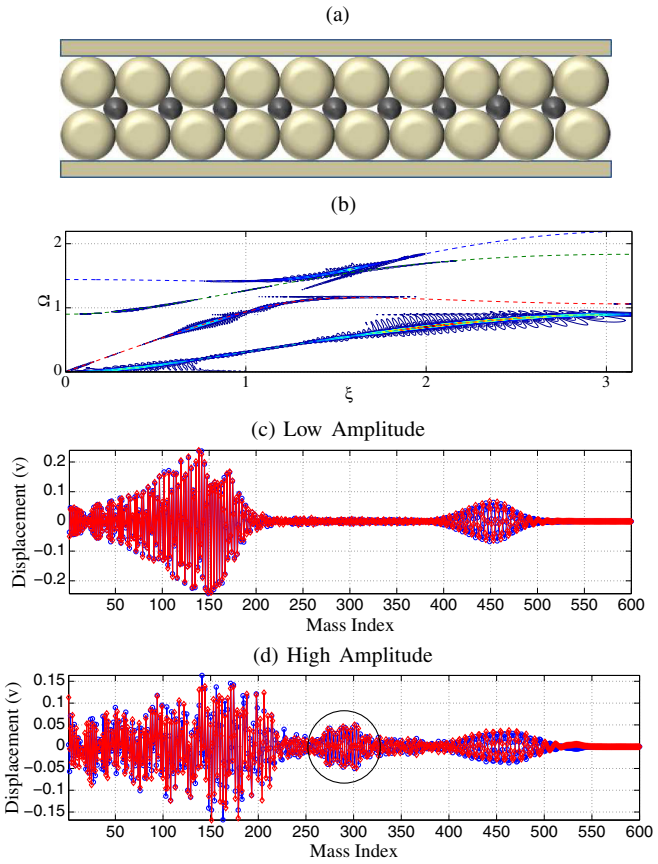

FIG. 3 (color online). Mode hopping and modal mixing in a granular waveguide. (a) Square-packed granular waveguide with interstitial inclusions. (b) Spectra of response for high-amplitude excitation superimposed on the linearized dispersion relation. (c), (d) Lateral wave profile for two different amplitudes of excitation displaying additional flexural features due to mode hopping. The excitation frequency is normalized by the linearized resonance frequency.

Here, the existence of two acoustic modes implies that even the fundamental harmonics propagate with multimodal characteristics featuring a mixture of axial and flexural deformation [Fig. 3(c)]. As the amplitude is increased, the optical modes corresponding to the second harmonic are also activated. Since the dominant optical mode shape involves primarily vertical displacement of the masses, we observe an additional burst of lateral displacement in the propagating packet, which travels at an intermediate speed between those of the acoustic modes. The lateral displacement profile, shown in Fig. 3(d), features three distinct oscillatory contributions in the wave profile - two corresponding to the incident acoustic excitation and one corresponding to the nonlinearly generated harmonic with optical mode characteristics. Therefore, this system effectively functions as a longitudinal-flexural energy converter, where large amplitudes of excitation trigger the activation of optical modes with pronounced flexural characteristics, thus inducing a net

energy transfer from longitudinal to flexural motion. This system can be envisioned as the logical building block of an amplitude filter in which the energy of high-amplitude excitations is rerouted laterally away from the main waveguide direction.

Our next example addresses the use of nonlinearity as a means to control spatial directivity in two-dimensional crystals. To this end, we consider the classical hexagonally packed 2D GPC depicted in Fig. 4, in which, for simplicity, all the beads are made of the same material and the confining loads are applied such that all the beads experience the same net precompression. In our simulations, the system is excited in the vertical direction by applying a narrow-band tone burst to the middle bead of the bottom layer. The dispersion characteristics of 2D crystals are described by phase constant surfaces, which relate the temporal frequency to the two components of the wave vector. For our purposes here, the modal structure of the crystal is fully captured by sampling the phase constant surfaces along the contour of the irreducible Brillouin zone, depicted in the band diagram of Fig. 4(b), in which we recognize two acoustic branches characterized by longitudinal- and shearlike deformation, respectively. For low-frequency excitations falling in the range of the acoustic branches (e.g., $\Omega = 1$), the longitudinal and shear modes coexist in the response, as suggested by the band diagram of Fig. 4(b). This is indeed reflected in the ξ-plane representation of the response depicted in Fig. 4(a), in which we plot spectral lines of the computed spatial response at a selected instant of propagation, superimposed to the isofrequency contours of the first two phase constant surfaces evaluated at the excitation frequency. We recognize the spectral signature of a faster, long-wavelength longitudinal mode with isotropic characteristics and a slower, short-wavelength shear mode that is directional with the classical sixfold symmetry of triangular lattice topologies [Fig. 4(a)]. The bimodal response is also verified from the spatial response shown in Fig. 4(d), in which the color map reflects the radial component of displacement.

As we increase the amplitude of excitation, we excite a second harmonic that lies on the longitudinal branch in a frequency range that is above the cutoff of the shear branch (along most of the contour of the irreducible Brillouin zone). Thus, the second harmonic provides an additional contribution to the longitudinal deformation of the crystal that has shorter wavelength and lower group velocity than the one excited by the fundamental harmonic. The ξ-plane representation of the response [Fig. 4(c)] indicates that this contribution features a directional behavior with a sixfold symmetry that is rotated by 45° with respect to that of the shear mode. The wave field shown in Fig. 4(e) confirms the presence of three distinct wave packets in the response:

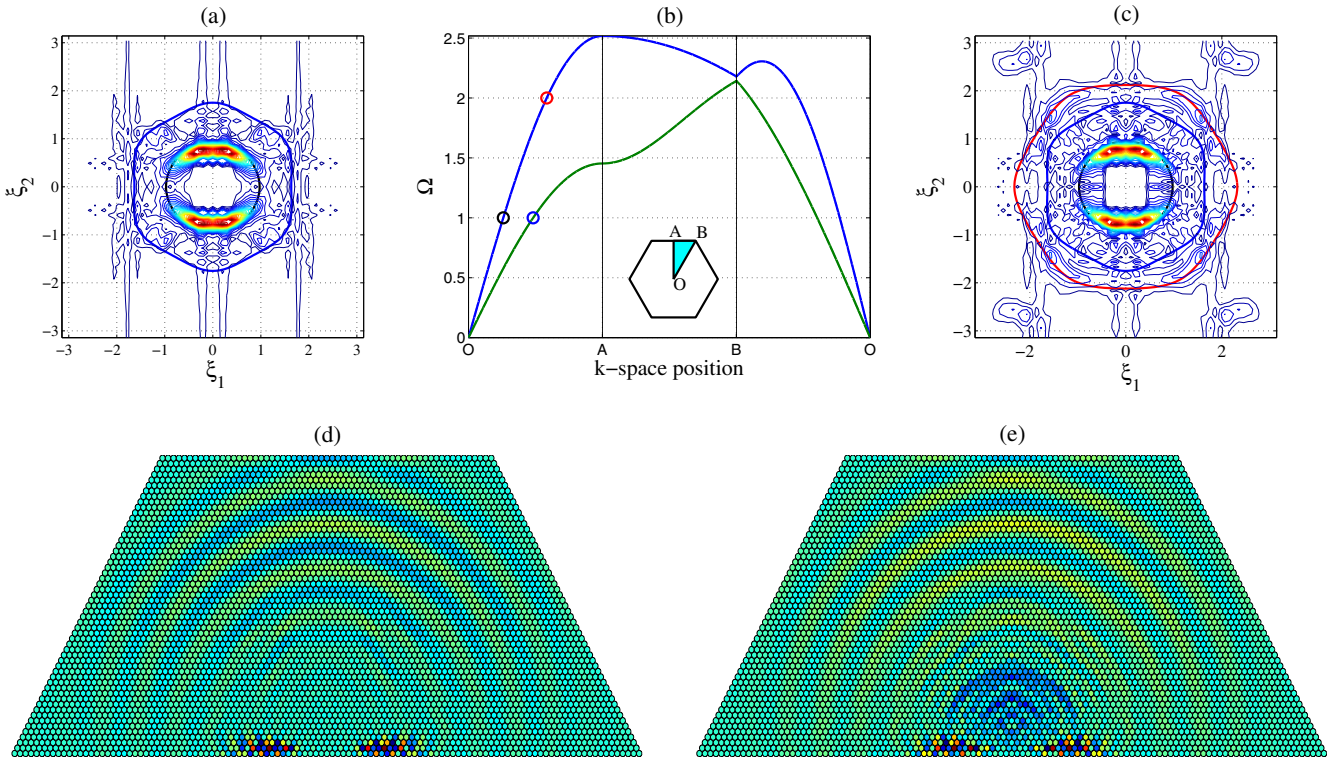

FIG. 4 (color online). Mode hopping and modal mixing in 2D crystals. (a),(c) Spatial Discrete Fourier Transform of the wave field highlighting the activation of different modal mixtures and different directionality patterns depending on the amplitude of excitation. (b) Band diagram calculated along the contour of the irreducible Brillouin zone. (d),(e) Wave field snapshots for the two amplitude values considered in (a) and (c), respectively.

the original acoustic modes seen in Fig. 4(d) and a new slower longitudinal mode with pronounced directional characteristics. By increasing the amplitude of excitation and triggering the second harmonic, we change the modal mixture of the response in a way that globally favors longitudinal mechanisms and also modify the directivity of the crystal by activating new directional paths that are normally experienced by the crystal at higher frequencies of excitation.

In conclusion, we have discussed a strategy to obtain spatial and modal wave manipulation in nonlinear phononic crystals using the concepts of mode hopping and modal mixing. We have shown that the generation of higher harmonics induces jumps in the response across the available propagation modes, thereby giving rise to a response with a mixture of modes and the simultaneous activation of complementary functionalities. As a result, functionalities that are normally associated with high-frequency modes can be activated in the response even while applying low-frequency excitations. The reversible activation and deactivation of strongly nonlinear conditions can be obtained either via external parameter tuning or as a spontaneous response to changes in the amplitude of excitation. The topological complexity of the crystal and the nature of nonlinearity ultimately determine the available opportunities for mode hopping and modal mixing, along with the landscape of functionalities that can be activated, thereby enabling access to virtually endless opportunities to engineer materials with desired tunable and switchable functionalities.

*ramak015@umn.edu
†sgonella@umn.edu

[1] M. S. Kushwaha, P. Halevi, L. Dobrzynski, and B. Djafari-Rouhani, Phys. Rev. Lett. **71**, 2022 (1993).
[2] R. Martínez-Sala, J. Sancho, J. V. Sánchez, V. Gómez, J. Llinares, and F. Meseguer, Nature (London) **378**, 241 (1995).
[3] A. S. Phani, J. Woodhouse, and N. A. Fleck, J. Acoust. Soc. Am. **119**, 1995 (2006).
[4] S. Gonella and M. Ruzzene, J. Sound Vib. **312**, 125 (2008).
[5] A. Spadoni, M. Ruzzene, S. Gonella, and F. Scarpa, Wave Motion **46**, 435 (2009).
[6] P. Celli and S. Gonella, J. Sound Vib. **333**, 114 (2014).
[7] M. Romanoni, S. Gonella, N. Apetre, and M. Ruzzene, Smart Mater. Struct. **18**, 125023 (2009).
[8] K. Bertoldi and M. C. Boyce, Phys. Rev. B **77**, 052105 (2008).
[9] P. Wang, F. Casadei, S. Shan, J. C. Weaver, and K. Bertoldi, Phys. Rev. Lett. **113**, 014301 (2014).
[10] S. Shan, S. H. Kang, P. Wang, C. Qu, S. Shian, E. R. Chen, and K. Bertoldi, Adv. Funct. Mater. **24**, 4935 (2014).
[11] A. Merkel, V. Tournat, and V. Gusev, Phys. Rev. E **82**, 031305 (2010).
[12] C. Daraio, V. Nesterenko, E. Herbold, and S. Jin, Phys. Rev. E **72**, 016603 (2005).
[13] C. Coste, Phys. Rev. E **77**, 021302 (2008).
[14] N. Boechler, G. Theocharis, S. Job, P. G. Kevrekidis, M. A. Porter, and C. Daraio, Phys. Rev. Lett. **104**, 244302 (2010).
[15] A. Merkel, V. Tournat, and V. Gusev, Phys. Rev. Lett. **107**, 225502 (2011).
[16] A. Leonard and C. Daraio, Phys. Rev. Lett. **108**, 214301 (2012).
[17] A. Leonard, C. Chong, P. G. Kevrekidis, and C. Daraio, Granular Matter **16**, 531 (2014).
[18] A. Spadoni and C. Daraio, Proc. Natl. Acad. Sci. U.S.A. **107**, 7230 (2010).
[19] N. Boechler, G. Theocharis, and C. Daraio, Nat. Mater. **10**, 665 (2011).
[20] C. M. Donahue, P. W. J. Anzel, L. Bonanomi, T. A. Keller, and C. Daraio, Appl. Phys. Lett. **104**, 014103 (2014).
[21] R. K. Narisetti, M. J. Leamy, and M. Ruzzene, J. Vib. Acoust. **132**, 031001 (2010).
[22] R. K. Narisetti, M. Ruzzene, and M. J. Leamy, Wave Motion **49**, 394 (2012).
[23] R. Ganesh and S. Gonella, Wave Motion **50**, 821 (2013).
[24] R. Ganesh and S. Gonella, Phys. Rev. E **90**, 023205 (2014).
[25] M. Remoissenet, *Waves Called Solitons*, Advanced Texts in Physics (Springer, Berlin, 1999).
[26] G. Huang, Z.-P. Shi, and Z. Xu, Phys. Rev. B **47**, 14561 (1993).
[27] V. J. Sánchez-Morcillo, I. Pérez-Arjona, V. Romero-García, V. Tournat, and V. E. Gusev, Phys. Rev. E **88**, 043203 (2013).
[28] J. Cabaret, V. Tournat, and P. Béquin, Phys. Rev. E **86**, 041305 (2012).
[29] K. L. Manktelow, M. J. Leamy, and M. Ruzzene, Wave Motion **51**, 886 (2014).
[30] See Supplemental Material at http://link.aps.org/supplemental/10.1103/PhysRevLett.114.054302 for modeling details, which includes Ref. [31].
[31] J. Dancz and S. A. Rice, J. Chem. Phys. **67**, 1418 (1977).